Available online at www.sciencedirect.com

SciVerse ScienceDirect

Energy Procedia 12 (2011) 1049 – 1056

Energy Procedia

ICSGCE 2011: 27–30 September 2011, Chengdu, China

Energy Conversion Stage Design of Solar Water Pump in a Nanofiltration System

Chuanlin Jin, Bingxing Wang, Dongliu Jiang, Wei Jiang*

Smart Energy Laboratory, School of Energy and Power Engineering, Yangzhou University, Yangzhou, China

Abstract

Standalone solar power system provides simple yet flexible solution to certain applications which demand high mobility. This paper introduces the design of a single solar panel powered induction machine-driven water pump system, which is used in an on-board nanofilteration system. The system configuration is evaluated at the first stage to provide high ratio voltage step-up; and complementary PWM and space vector PWM scheme is chosen for dc-dc stage and dc-ac stage respectively; V/F based control scheme is designed and integrated with maximum power point tracking algorithm for the best use of solar panel. The control system is implemented digitally in a TMS320F2812 DSC. Meaningful mode of operation is tested and satisfactory experimental results are collected.

Selection and/or peer-review under responsibility of University of Electronic Science and Technology of China (UESTC)

Keywords: Solar energy, water pump, digital control, induction motor drive

1. Introduction

Solar is one of the most environment-friendly renewable energy sources. The process of solar energy generation required no extra energy input and yields no harmful emissions. Therefore, solar energy is considered as one of the most important primary energy sources in the future.

Even today, some remote areas cannot be covered by the utility grid; however, most of those areas are of abundant sun illumination. Therefore, standalone power system will be quite suitable for those regions. Generally, there are two solutions for the standalone power system, one is micro-grids based, in which the renewable energy sources are connected to a common dc or ac bus via power electronic converters. The electric/electronic appliances and equipments within the grid area can be fed with high quality electric power using power electronic converters. Micro-grids based solution requires huge transmission and distribution infrastructure investment, which is indeed a “micro” version of current utility grid. The other

* Corresponding author. Tel.: +86-514-87971315.
E-mail address: jiangwei@yzu.edu.cn.

doi:10.1016/j.egypro.2011.10.137

solution is non-grid based, in which one source fed one load, for example. This solution offers high mobility and flexibility for different applications, for example solar powered water pumping for irrigation.

Water treatment is of very importance for daily life. In such appliances, collected rain water is pumped via an induction machine driven water pump into a nanofiltration chamber, which delivers clean water for drinking. Due to the nature of this application, the water treatment appliance has to be highly mobile, so that only one photovoltaic panel and one fractional horse-power induction machine is used in the system.

This paper investigates the design and implementation of the energy conversion stage of a water pump system, which is sourced by one photovoltaic panel without any energy storage and loaded by one fractional horse-power induction machine (FHPIM). The system configuration is evaluated at the first stage to provide high ratio voltage step-up; and complementary PWM and space vector PWM scheme is chosen for dc-dc stage and dc-ac stage respectively; V/F based control scheme is designed and integrated with maximum power point tracking algorithm for the best use of solar panel. The control system is implemented digitally in a TMS320F2812 DSC, meaningful scenarios of operation is tested to prove the feasibility of the design.

2. Theory of Operation

As can be seen from Fig. 1, low power induction motor drive system consists of five interrelated parts: the photovoltaic array, dc-dc converter, dc-ac inverter, control module and the pump.

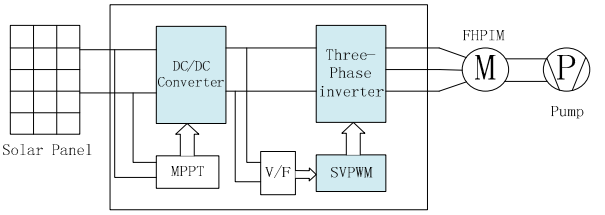

Fig. 1. System Structure.

The power flow from the solar panel has to be maximized and boosted to supply the DC bus of IM drive system. A market research has been conducted on the off-the-shelf solar panels; the panels which deliver 120-150W usually have open circuit voltage V_{OC} of 21V to 42V, hence the V_{MPP} can be estimated. In order to run a 220VAC induction motor, a DC bus of 350V is required considering the safety margin. Therefore the front-end converter has to boost the input voltage with a large ratio. An isolated dc-dc topology is used as our front-end converter: single phase full bridge + HF transformer + half bridge rectifier. S_1 and S_2 are switched above 50% duty cycle with 180 degree phase shift at 50 kHz, S_4 and S_3 are switched below 50% duty with 180 degree phase shift, D_1 and D_2 together with two series connected capacitor form a voltage doubler for dc output.

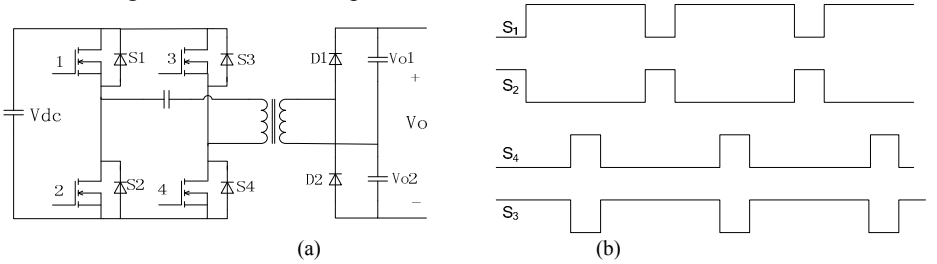

Fig. 2. dc-dc converter (a) schematics; (b) PWM logic.

Photovoltaic array has output characteristics of nonlinearality obviously, which are affected by external environment (sunshine intensity, temperature and load) and itself technical index (output resistance). Only at a voltage, photovoltaic array can output maximum power, and then the photovoltaic array reaches the highest point of power output voltage curve, called "the Maximum Power Point". Currently the conversion efficiency of photovoltaic array is rather low, and for effective use, Maximum Power Point Tracking (MPPT) appears very important. In this study, the Perturbation and Observation method (P&O) is used to track the MPP, the principle of which is described below.

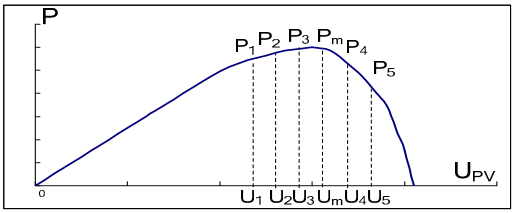

Fig. 3. P&O MPPT Principle.

Imagine the work point is at U_1 now, the output power is P_1 at this moment, if we move the work point to $U_2 = U_1 + \Delta U$, output power would be P_2, compare P_2 with P_1, if $P_2 > P_1$, it means the input signal difference amplifies the output power, work point locates left to P_m, we need to increase the voltage to move the work point towards P_m; if the work point has already crossed Pm to U_4, and increase the voltage to U_5, if the result of comparison is $P_5 < P_4$, it means the work point locates right to P_m, we should reverse the change direction of input signal, and compare current power with previous power to find P_m.

Variable voltage and variable frequency (VVVF) is selected as the means for power regulation. The control block of the system is shown in Fig. 4. The estimated solar panel V_{MPP} is used as the reference for the VVVF control loop, the resulted error is fed into a PI controller to generate an excitation frequency; the output stator voltage of IM can be obtained by look-up V/F table; the generated voltage reference value is used in SVPWM generator for six gate pulses.

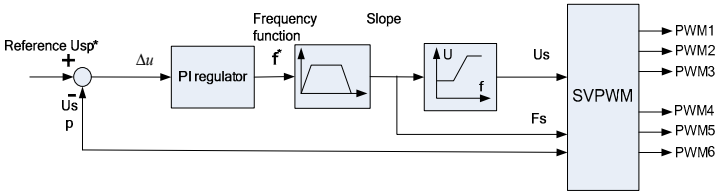

Fig. 4. VVVF control of induction motor

3. Power Stage Design

The panels which deliver 120-150W usually have open circuit voltage V_{OC} of 21V or 42V, so we suppose the power of the panels is 150W and the open circuit voltage *Voc* is 30V. The panel current can be calculated as 5A through $I=P/U$. The duty of PWM which control the MOSFET is 80%, so we can calculate that the max-current through the MOSFET is 6.25A through $I_{max}=I/0.8$. On this basis, IRF540, of which I_d is 33A and V_{ds} is 100V, is chosen as the inverter switch. The dc system should at least offer a voltage gain of 16 in order to take care of very low solar panel input (20V). Therefore, using the half bridge rectifier secondary, the ratio is chosen as n=8, therefore we set the turn ratio 13:100. At the secondary side, as the voltage level is 350V, and power is about 150W, the maximum current is 0.43A,

therefore fast recovery diode ES1J is sufficient for this application, which average current is 1A. In dc-ac inverter circuit, IPM FSBS5CH60 is chosen as the power stage for the three phase inverter. It is an advanced smart power module (SPMTM) that Fairchild has newly developed and designed to provide very compact and high performance ac motor drives mainly targeting low power inverter-driven application like air conditioner and washing machine. The supply voltage of IPM FSBS5CH60 is 500V, which can satisfy our dc link voltage of 350V, and 5A output current is sufficient for the solar pump application. It combines optimized circuit protection and drive matched to low-loss IGBTs. System reliability is further enhanced by the integrated under-voltage lock-out and short-circuit protection. The high speed built-in HVIC provides optocoupler-less single-supply IGBT gate driving capability that further reduce the overall size of the inverter system design. Each phase current of inverter can be monitored separately due to the divided negative dc terminals.

4. Control Circuit Design

The isolated sampling circuit is adopted as the voltage and current sensing circuit. The advantages of this sampling circuit are: +5 V power supply only; the main circuit and control circuit are isolated by HCPL7800 isolation amplifier, thereby the control circuit can be protected. Here we need to sample the voltage and current of the dc bus, the inverter input and output dc bus voltage, and the output current. Then we can achieve MPPT and VVVF control by processing these sampled voltages and currents.

The solar panel output voltage is converted to 10V first to supply the control peripherals using a LM2596 simple switcher. The 10V is output is then converted to 15V for the gate drive and other supporting circuit. The reason for this design is that the solar panel voltage will fluctuate during the test, if solar panel voltage drops down below 15V, the power stage will lose power supply. Therefore Vin-10V-15 structure is chosen for reliability considerations. For safety consideration, we use the method of opto-isolation to isolate the drive circuit and the control circuit.

5. Algorithm Design

Local control includes PWM, SVPWM modulation and VVVF control. Eight PWM signals are needed to drive the power stage as indicated in the hardware design. Two of them are used to gate the MOSFET of full bridge dc-dc converter and the other six are used to the IPM.

As indicated in Fig.5, the generation method is stated below:

Step 1: Determine *Vref*, and angle (α);

Step 2: Determine time duration *T1*, *T2*, *T0*;

Step 3: Determine the switching time of each IGBT (S_1 to S_6).

To implement the *V/f=C* control, two variables have to be adjusted: *V* and *f*. And

$$\frac{m}{\Delta\theta} = \frac{V}{f} = C \tag{1}$$

in this equation *m* is the amplitude modulation index and $m=V/V_{dc}$, V_{dc} is the input voltage of inverter. $\Delta\theta$ is the angle of phase voltage vector's rotation increment, which is modified during each PWM underflow interrupt during DSC operation. The vector rotation increment and rotation angel is given as

$$\Delta\theta = \frac{2\pi f}{T_{pwm}} \tag{2}$$

$$\theta = \theta + \Delta\theta \tag{3}$$

where θ is the angle of vector V_1 in the reference frame, f is the output voltage frequency. So we just need to introduce m and $\Delta\theta$ during the software interrupt for a V/F control. If we want to increase the speed of motor, or to increase f, which means just make θ change quickly, we can let $\Delta\theta = \Delta\theta + 1$. Conversely, we let $\Delta\theta = \Delta\theta - 1$ in the DSC register. At the mean time, m is also modified in SVPWM service routine; so that V/F is keep constant while changing the motor speed.

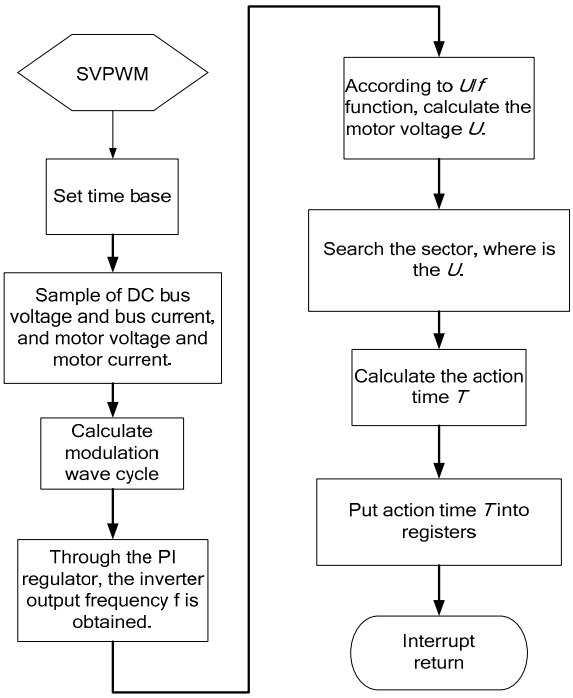

Fig. 5. Flowchart of SVPWM interrupt subroutine.

If f is increased, the output power of motor will be increased, so the output power of photovoltaic panel will also be greater, conversely, if f is decreased, output power will be decreased too, and the output power of photovoltaic panel will drop. Therefore, the output power of the IM should be adjusted constantly in order to keep the output power of photovoltaic panel staying in the MPP. Because the output power of pump motor is proportional to speed's cube, and speed is proportional to the input voltage, so the output power of the pump is proportional to its input voltage.

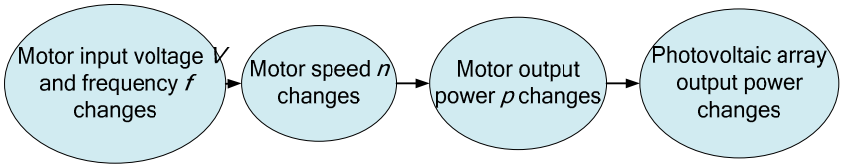

Fig. 6. Principle of power control.

As indicated in Fig. 6, if *V/F* is kept constant in SVPWM algorithm, the output power can be adjusted by changing the excitation frequency. So photovoltaic array's load matching can be realized by changing the speed of the pump. Namely through speed reference regulation, we can adjust the photovoltaic array's output load, and make the output power follow the maximum power point of the solar panel all the time.

6. Testing Results

The induction machine test bed is indicated in the Fig.7, the initial test is conducted in an indoor lab environment. As can be seen in Fig.7, the system includes a regulated power supply, which output voltage is from 20V to 40V adjustable during the test, an embedded F2812 control board, a power board for the solar pump converter and a FHPIM of 120W, three phase 220VAC input.

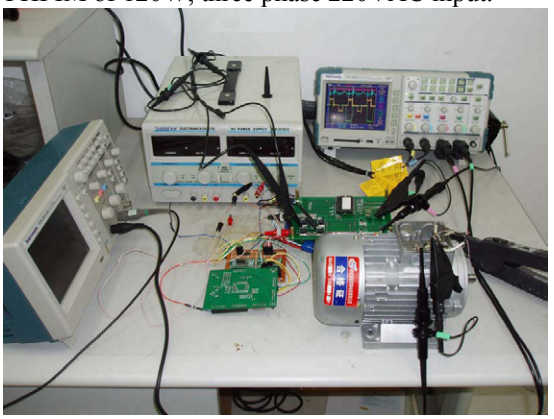

Fig. 7. Test bed with 120W IM.

The input voltage is initially set at 24VDC and 300V plus dc voltage can be obtained on the system dc-link. The test is conducted with constant V/F ratio for 220VAC/50Hz, different amplitude modulation index is selected for test purpose as shown in the figure below. Under four different speed tests, the system presents excellent electrical and thermal stability. The system is tested under different excitation frequency; two of the tests are indicated in Fig. 8 and Fig. 9. As can be seen in the figure, CH1 shows the transformer primary voltage of 24V (yellow curve, 1V/div, 10X attenuated) which is supplied by a dc power supply. The CH2 (blue curve, 1V/div, 10X attenuated) standing for the input voltage from the dc power supply, which emulates the solar panel output. The dc link voltage (CH3, purple curve, 100V/div) is the output voltage from the dc-dc converter and the input of dc-ac inverter. CH4 (green, 100V/div) stands for the inverter output which is regulated in open loop as the modulation index *m* is under change. The experimental results shows that as the solar panel voltage is regulated, the speed of IM changes. Fig. 8 shows the input/output waveforms of the power stage at the modulation index of 0.8 and 50Hz of excitation frequency, and Fig. 9 shows the input/output waveforms for m=0.5m, f=31.25Hz.

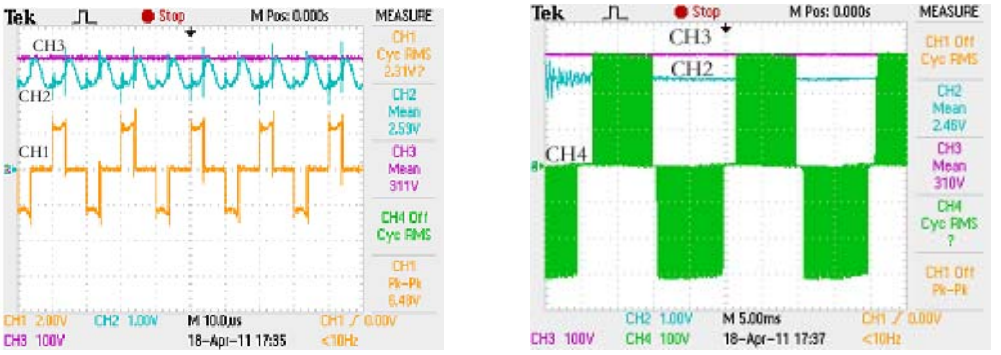

(a) (b)

Fig. 8. Test waveforms under m=0.8 f=50.00Hz with 120W IM, (a) system input; (b) system output

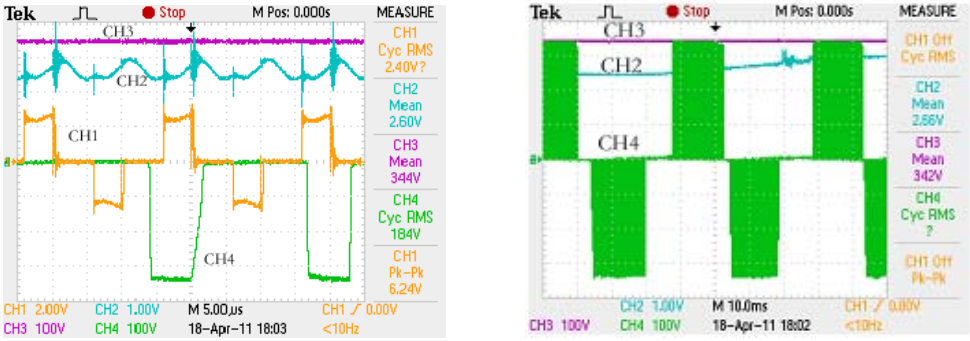

(a) (b)

Fig. 9. Test waveforms under m=0.5 f=31.25Hz with 120W IM, (a) system input; (b) system output

7. Conclusion

This paper presents the energy conversion stage design for a solar powered water pump system in a nanofiltration system. The system configuration, PWM algorithm, control system structure and power stage hardware design are presented in detail. The control system is implemented in a TMS320F2812 DSC and tested in several meaningful modes of operation. The test results indicated the effectiveness of the system design and digital control implementation.

Acknowledgment

The authors would like to thank the financial support from the Dean's Office of School of Energy and Power Engineering, Provost Office of Yangzhou University, and Undergraduate Student Innovation Funding grant.

References

[1] Montesinos-Miracle, Daniel, A new low-cost DSP educational tool for a laboratory for motor control. International Journal of Electrical Engineering Education, v 46, n 2, 2009,pp. 183-197.

[2] Guo, Junmei, DSP practical solutions for motor control using DSP-controller. 2010 International Conference on Networking and Digital Society, ICNDS 2010,v 2,2010, pp. 629-632.

[3] Shireen, Wajiha, Laboratory setup for variable speed control of a three phase AC induction motor using a DSP Controller. ASEE Annual Conference Proceedings, 2002, pp. 7983-7987.

[4] Matsui, Nobuyuki, DSP-based intelligent motor/motion control. Proceedings of the American Control Conference, v 1, 1995, pp. 490-494.

[5] Pfile, Richard E. ,Using a DSP controller to control a three-phase induction motor. ASEE Annual Conference Proceedings, 1999, pp. 5489-5497.

[6] Poshtkouhi, Shahab, Multi-input single-inductor DC-DC converter for MPPT in parallel-connected photovoltaic applications. Conference Proceedings - IEEE Applied Power Electronics Conference and Exposition - APEC, 2011, pp. 41-47.

[7] Cheng, Ze, Self-adjusting fuzzy MPPT PV system control by FPGA design. 2011 Asia-Pacific Power and Energy Engineering Conference, APPEEC 2011 - Proceedings, 2011.

[8] Durgadevi, A. , Study and implementation of Maximum Power Point Tracking (MPPT) algorithm for Photovoltaic systems. 2011 1st International Conference on Electrical Energy Systems, ICEES 2011,2011, pp. 240-245.

[9] Qiu, Pei-Chun, MPPT control for PV power generation system based on P&O algorithms and quadratic interpolation. Dianli Xitong Baohu yu Kongzhi/Power System Protection and Control, v 39, n 4, 2011, pp. 62-67.

[10] Spiazzi, G., Low complexity MPPT techniques for PV module converters. 2010 International Power Electronics Conference - ECCE Asia -, IPEC 2010, 2010, pp. 2074-2081.

[11] Nagayoshi, Hiroshi, Development of 100-W high-efficiency MPPT power conditioner and evaluation of TEG system with battery load. Journal of Electronic Materials, v 40, n 5,2011, pp. 657-661.

[12] Lapsley, P. ,DSP Processor Fundamentals : Architectures and Features. Wiley-IEEE Press. 1997.

[13] Lars Wanhammar, DSP Integrated Circuits. 1999

[14] Nivedita Dasgupta, Voltage-sensing-based photovoltaic MPPT with improved tracking and drift avoidance capabilities. Solar Energy Materials and Solar Cells, Volume 92, Issue 12, 2008, pp. 1552-1558.

[15] A. Mellit, H., FPGA-based real time implementation of MPPT-controller for photovoltaic systems. Renewable Energy, Volume 36, Issue 5, 2011, pp.1652-1661.

[16] M. K. Maaziz, A new nonlinear multivariable control strategy of induction motors. Control Engineering Practice, Volume 10, Issue 6, 2002, pp. 605-613.

[17] Fayez G. Areed, Adaptive neuro-fuzzy control of an induction motor.Ain Shams Engineering Journal, Volume 1, Issue 1, 2010, pp. 71-78.

[18] Jinpeng Yu, Position tracking control of induction motors via adaptive fuzzy backstepping. Energy Conversion and Management, Volume 51, Issue 11, November 2010, pp. 2345-2352.

[19] Romeo Ortega, On speed control of induction motors. Automatica, Volume 32, Issue 3, March 1996, pp. 455-460.

[20] Metin Demirtas, DSP-based sliding mode speed control of induction motor using neuro-genetic structure. Expert Systems with Applications, Volume 36, Issue 3, Part 1, April 2009, pp. 5533-5540.

[21] M.N. Cirstea, Neural current and speed control of induction motors. Neural and Fuzzy Logic Control of Drives and Power Systems, 2002, pp. 159-236.

[22] Keith H. Sueker, Power Electronics Design. 2005.

[23] Bimal K. Bose, Power Electronics And Motor Drives. 2006.

[24] Muhammad H. Rashid, Ph.D., Power Electronics Handbook (Third Edition). 2011.